

THE MIXING EFFECT ON THE FREE RADICAL MMA SOLUTION POLYMERIZATION

Jae Youn Kim* and Robert L. Laurence†

Department of Chemical Engineering, University of Massachusetts, Amherst, MA 01003

(Received 29 August 1997 • accepted 7 April 1998)

Abstract – Mathematical models of reactors for the polymerization of methylmethacrylate (MMA) have been developed and analyzed to elucidate reactor dynamics and to determine conditions for improved operation. The effects of mixing and heat transfer in an MMA polymerization reactor system have been explored by the development of an imperfect mixing model. To model imperfect mixing in polymerization, a reactor configuration using two tanks in parallel was used. Bifurcation diagrams developed using numerical analysis of the model have been drawn with two variable parameters, an exchange ratio, σ , and a volume ratio, κ . We use feed and coolant temperatures as bifurcation parameters. If variable parameters are small, the lower solution branch of the steady state solutions is quite different from that of a simple model that assumes perfect macro-mixing as bifurcation parameters change. If σ increases ($\kappa=0.1$, $\sigma=1.0$), the shape of a steady state solution curve differs significantly from that of a simple model as the feed temperature decreases.

Key words : Reactor, Dynamics, Bifurcation, Polymerization, Solution

INTRODUCTION

Mixing of the reaction mixture in the polymerization reactor is very important. Since the polymerization of MMA is also highly exothermic, some hot spots as well as thermal runaway may occur if the mixing of the mixture is poor. Polymer properties may also change due to poor mixing. The degree of polymerization in the hot spot may increase significantly. However, most researchers [Adebekun et al., 1989; Choi, 1986; Kwalik, 1988; Kiparissides et al., 1990] studying the process for the polymerization of methylmethacrylate (MMA) assumed perfect mixing to derive the equations for mass and energy balances in the reactor.

The large increase in viscosity with monomer conversion is one of the important phenomena of polymerization reactions that has a very significant effect on heat and mass transfer in reaction mixtures and on the apparent polymerization kinetics. The increase in viscosity leads to diffusion limitation of the termination reaction, resulting in an accelerated polymerization and an increase in heat generation [Moritz, 1989]. If the reaction mixture is not well mixed, some regions in the reactor may have hot spots (with temperature runaway) or may become dead zones in which the flow and reaction differ from the rest of the reactor. Thiele [1989] studied the interaction between process design and mechanical design in mass polymerization reactors. He noted that local mixing and overall mixing characteristics of the reactor are related to stirrer construction and choice of mixer speed. He

compared a perfect micromixing model and a segregation model, noting that neither is adequate. Tosun [1992] used the segregated mixing model developed by Villermaux [1989] to derive a mathematical model of mixing in a semi-batch polymerization reactor. He showed that weight average degree of polymerization is strongly affected by mixing conditions. Thiele and Breme [1988] found that a segregation model is appropriate for the system at low agitation speeds, and a perfect micromixing model for high speeds. Chen and Fan [1971] modeled complete segregation by the convolution of the batch reactor states with the residence time distribution; this is called the environment model. Villermaux [1986] introduced interaction-by-exchange-with-the-mean (IEM) model by assuming that the reactor fluid consists of many elements in which a large number of molecules are contained. The model is based on a population balance over element properties. Such a model is called the fluid particle model. A serious drawback of these two models, however, is that they can be applied only to isothermal systems. In a study of macromixing in a CSTR with two inlet streams Kaflas [1992] used a fluid flow model in which the existence of two mixing zones formed by the flow patterns is assumed, where mass is exchanged at a rate which depends on the reaction mixture, the intensity of mixing, the reactor size, etc. He showed the effect of recycle ratio and volume ratio on the polydispersity of polymer product and conversion of monomer, but did not study the reactor dynamics. The models described above contain several parameters to explain the real mixing phenomena of polymerization reactors. These parameters depend strongly on the type of reactor and mixing device.

Here, we assume two mixing zones in a CSTR for polymerization of MMA. The two exchange mass and energy. A schematic diagram of this model is shown in Fig. 1, where

*To whom all correspondence should be addressed.

†Current Address : Chemicals Research Division, Hanwha Group R/E Center, Taejon, 305-345, Korea
E-mail : jaekim@indigo2.hanwha.co.kr

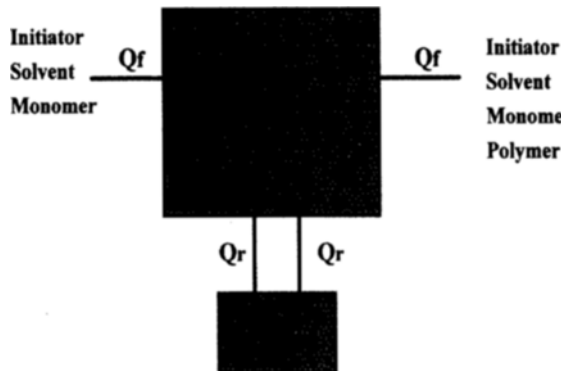


Fig. 1. Schematic diagram of two-tank-in-parallel reactor system.

the reactor vessel was assumed to consist of two zones: a small zone surrounding the impeller and a large one occupying the remaining tank volume. Two important parameters, that is, the volume ratio, κ , and the exchange ratio, σ , are used to study the sensitivity of reactor dynamics to operating parameters. We use feed and coolant temperatures as bifurcation parameters.

THE EQUATIONS GOVERNING THE POLYMERIZATION

To derive material and energy balances for various species in the two tank-in-parallel shown in Fig. 1, we use the same assumptions described in the introduction section. The Trommsdorff effect included is the Ross-Laurence correlation. The

Table 1. Governing equations of the two-tank-in-parallel model

$V_1 \frac{dM_1}{dt} = q_f M_f + q_r M_2 - q_f M_1 - q_r M_1 - V_1 k_p M_1 \lambda_1$	$V_1 \frac{dI_1}{dt} = q_f I_f + q_r I_2 - q_f I_1 - q_r I_1 - V_1 k_d I_1$
$V_1 \frac{dS_1}{dt} = q_f S_f + q_r S_2 - q_f S_1 - q_r S_1$	$V_1 \frac{dT_1}{dt} = \rho C_p (q_f T_f + q_r T_2 - q_f T_1 - q_r T_1) + (-\Delta H_p) V_1 k_p M_1 \lambda_1 - U A_r (T_1 - T_c)$
$V_1 \frac{d\lambda_1}{dt} = q_r \lambda_2 - q_f \lambda_1 - q_r \lambda_1 + V_1 (2 f k_d I_1 - k_r \lambda_1^2)$	$V_1 \frac{dM_2}{dt} = q_r M_1 - q_r M_2 - V_2 k_p M_2 \lambda_2$
$V_2 \frac{dI_2}{dt} = q_r I_1 - q_r I_2 - V_2 k_d I_2$	$V_2 \frac{dS_2}{dt} = q_r S_1 - q_r S_2$
$V_2 \frac{dT_2}{dt} = \rho C_p (q_r T_1 - q_r T_2) + (-\Delta H_p) V_2 k_p M_2 \lambda_2$	$V_2 \frac{d\lambda_2}{dt} = q_r \lambda_1 - q_r \lambda_2 + V_2 (2 f k_d I_2 - k_r \lambda_2^2)$

*Subscripts 1 and 2 denote the first tank and the second tank, respectively.

* λ_1 and λ_2 denote λ_0 in the first tank and in the second tank, respectively.

system equations are shown in Table 1. The dimensionless groups used to restate the governing equations are depicted in Table 2. Two parameters are included in addition to those in the modified simple model—the flow exchange ratio, σ , and the reactor volume ratio, κ . If σ is sufficiently large, the imperfect mixing model becomes the modified simple model. If σ is sufficiently small, the mixing in the reactor is poor and the ideal mixing model may not express the real dynamics of the reactor. If κ becomes one, it may show that the dynamics of the two reactors are linked in parallel. The volume of each is half the reactor used in the modified simple model. This imperfect mixing model is used to describe the effect of macro-mixing on reactor dynamics. Several different methods, such as an environment model and a fluid particle model, have been used to describe micromixing in a reactor. Neither model may be readily adapted to nonisothermal processes. The calculation or measurement of the temperature and concentration histories of microscale elements is not a tractable problem. The polymerization of MMA is highly exothermic. Here, we use an imperfect mixing model to study the effect of mixing on reactor dynamics. The physical properties of materials and kinetic constants are shown in Table 3 and 4, respectively. Reactor and reactor medium

Table 2. Dimensionless groups for the two-tank-in parallel model

$\tau = \frac{t q_f}{V_1} = \frac{t}{\theta}$	$X_1 = \frac{M_f - M_1}{M_f}$	$X_2 = \frac{I_f - I_1}{I_f}$
$X_3 = \frac{S_f - S_1}{S_f}$	$X_4 = \frac{T_1 - T_f}{T_f} \gamma_p$	$X_5 = \frac{\lambda_1}{M_f}$
$X_6 = \frac{M_f - M_2}{M_f}$	$X_7 = \frac{I_f - I_2}{I_f}$	$X_8 = \frac{T_2 - T_f}{T_f} \gamma_p$
$X_9 = \frac{S_f - S_2}{S_f}$	$X_{10} = \frac{\lambda_2}{M_f}$	$\gamma_p = \frac{E_{p0}}{R T_f}$
$\gamma_p = \frac{E_{p0}}{E_{p0}}$	$\gamma_f = \frac{E_f}{E_{p0}}$	$X_C = \frac{(T_c - T_f)}{T_f} \gamma_p$
$BH = \frac{(-\Delta H_p) M_f}{\rho C_p}$	$\beta = \frac{U A_r}{\rho C_p q_f}$	$\kappa = \frac{V_2}{V_1}$
$\sigma = \frac{q_r}{q_f}$	$\eta = \frac{I_f}{M_f}$	$D_{ap} = \theta M_f k_{p0} \exp(-\gamma_p \gamma_f)$
		$D_{at} = \theta M_f K_{k0} \exp(-\gamma_p \gamma_f)$

Table 3. Physical properties of materials in the polymerization of MMA

$\rho_M = 0.968 - 1.255 \times 10^{-3} T_c$	(g/cm ³)
$\rho_p = \rho_M (1 + \epsilon)$	(g/cm ³)
$\epsilon = 0.183 + 9.0 \times 10^{-4} T_c$	
$\rho_s = 0.883 - 9.0 \times 10^{-4} T_c$	(g/cm ³)
$C_{PM} = 0.4$	(cal/g°C)
$C_{PP} = 0.339 + 9.55 \times 10^{-4} (T_c - 25)$	(cal/g°C)
$C_{PS} = 0.535$	(cal/g°C)
$M_{WM} = 100.13$	(g/mol)
$M_{WS} = 92.14$	(g/mol)
$(-\Delta H_p) = 13,800$	(cal/mol)

* T_c : T (°C)

Table 4. Kinetic constants for the MMA polymerization

$k_d = 6.32 \times 10^{16} \exp\left(-\frac{30.66(\text{kcal/mol})}{RT}\right)$	$\left(\frac{l}{\text{min}}\right)$
$k_p^0 = 2.95 \times 10^7 \exp\left(-\frac{4.35(\text{kcal/mol})}{RT}\right)$	$\left(\frac{l}{\text{min min}}\right)$
$k_{fM} = k_p \cdot 9.48 \times 10^3 \exp\left(-\frac{13.88(\text{kcal/mol})}{RT}\right)$	
$k_{fs} = k_p \cdot 1.01 \times 10^3 \exp\left(\frac{11.44(\text{kcal/mol})}{RT}\right)$	
$k_r^0 = 5.88 \times 10^9 \exp\left(-\frac{0.701(\text{kcal/mol})}{RT}\right)$	$\left(\frac{l}{\text{min min}}\right)$
$k_r = k_{rc} \cdot 3.956 \times 10^{-4} \exp\left(-\frac{4.09(\text{kcal/mol})}{RT}\right)$	
$k_r = k_{rc} + k_{kd}$	

Reference: Baillagou and Soong [1985]

Table 5. Isola centers for a modified simple model

$X_1=0.79391$	$X_2=0.25971$	$X_3=0.697169$	$X_4=0.667893$
$X_3=1.3615$	$X_4=1.0$	$X_3=1.93488$	$X_4=1.0$
$X_5=4.94999 \times 10^{-7}$	Model=Simple	$X_5=6.73771 \times 10^{-7}$	Model=Simple
$\theta=0.332036$		$\theta=0.0942569$	$T_F=312.326$
Reactor and reactor medium constants			
$f=0.8, U=135 \text{ cal/m}^2\text{sK}, Ar=2.8 \text{ m}^2$			

Fixed parameters: $I_F=0.05, M_F=5.0, S_F=4.7, T_C=T_F$

constants used to calculate the steady state solutions are shown in Table 5.

RESULTS AND DISCUSSION

Bifurcation analysis of autonomous systems is used to analyze the reactor dynamics of MMA polymerization. The governing equations are highly nonlinear and it is not possible to reduce the set to one equation. Uppal et al. [1974, 1976] and Balakotaiah and Luss [1982] applied bifurcation theory in their analysis of the dynamics of chemically reacting systems. They were able to reduce their equations to a single algebraic expression using the Liapunov-Schmidt method. Though multiple steady states and Hopf bifurcations may be derived analytically, this method is intractable for systems of large dimension. Doedel [1986] developed the software package AUTO by using numerical continuation. AUTO can be used to trace the steady solution branches, to detect static bifurcation points (multiple steady state solutions), and to compute the bifurcating branches. It also locates Hopf bifurcation points and traces periodic solution branches. In this work, we have used AUTO to analyze the reactor dynamics described by the equations in Table 4. In order to draw a bifurcation diagram, that is, a plot of a state of the system versus the main free parameter, we must select main parameters among a given parameter set. Hamer et al. [1981], Teymour and Ray [1989], and Adebekun et al. [1989] chose initiator feed concentration and feed solvent fraction as their main free parameters. Hamer et al. [1981] plotted the classification parameter space diagram using a nonlinear constrained optimization. In this diagram,

the space is divided into regions showing different bifurcation behavior. It describes the parametric sensitivity of reactor dynamics very well. However, some regions, where exotic phenomena such as Hopf bifurcations occur, may not be significant. For example, Teymour and Ray [1989] found two different bifurcation diagrams when initiator feed concentration decreased from 0.01345 (mol/l) to 0.01337 (mol/l). Such a small concentration difference, 8×10^{-5} (mol/l), is hard to control and impossible to measure.

The control of feed and coolant temperatures is also very important, since MMA polymerization is highly exothermic and an increase in reaction temperature may affect polymer properties. Kwalik et al. [1989] varied the feed temperature in their construction of bifurcation diagrams for a well-mixed polymerization reactor. Solvent volume fraction was used as another free parameter. They found multiple isola solution branches for specific parameter values. In this work, solvent concentration is used rather than solvent volume fraction as a fixed parameter. Concentration is more readily measured and the calculation of volume fraction requires molecular weight, density and concentration.

$$\phi_s = \frac{M_{ws}}{\rho_s} S_f$$

Residence time, θ , is used as a main parameter. Feed and coolant temperatures (T_f and T_c) are changed to construct bifurcation diagram for MMA polymerization in an imperfectly mixed CSTR. The values of the fixed parameters used are the same as those in Kwalik et al. [1989].

AUTO code uses a continuation method in which the computation begins at a known solution point and continues to points along a specific branch of solutions. Therefore, it cannot detect isola type solution branches without knowing a point on an isola. Several methods have been used to calculate isola solution branches. Kwalik [1988] used a root finding method to find multiple steady state solutions of the nonlinear governing equations for a fixed set of operating conditions. However, it is computation-intensive. Choi [1986] made use of the criteria developed by Balakotaiah and Luss [1982] and reduced his governing equations to one equation. His set of equations did not account for the gel effect. Kubicek and Marek [1983] developed a numerical algorithm for location of the point of formation of isola solution branches of nonlinear algebraic equations. It uses a necessary condition for the existence of a limit point. To detect the isola formation center, two free parameters are needed. Given an isola center, a slightly perturbed value of one of the free parameters is used to solve the system of governing equations by Newton's method. AUTO is then used to calculate isola solution branches by using the solution of nonlinear equations as initial solution points. Since the dimension of the governing equations is large, this algorithm has been adopted here.

1. Modified Simple Model

A modified simple model, which uses the perfect mixing assumption and excludes QSSA and removes the contribution of initiator volume fraction in Ross-Laurence empirical gel model [1976], has been calculated to afford a basis for comparison with the imperfect mixing model and to show

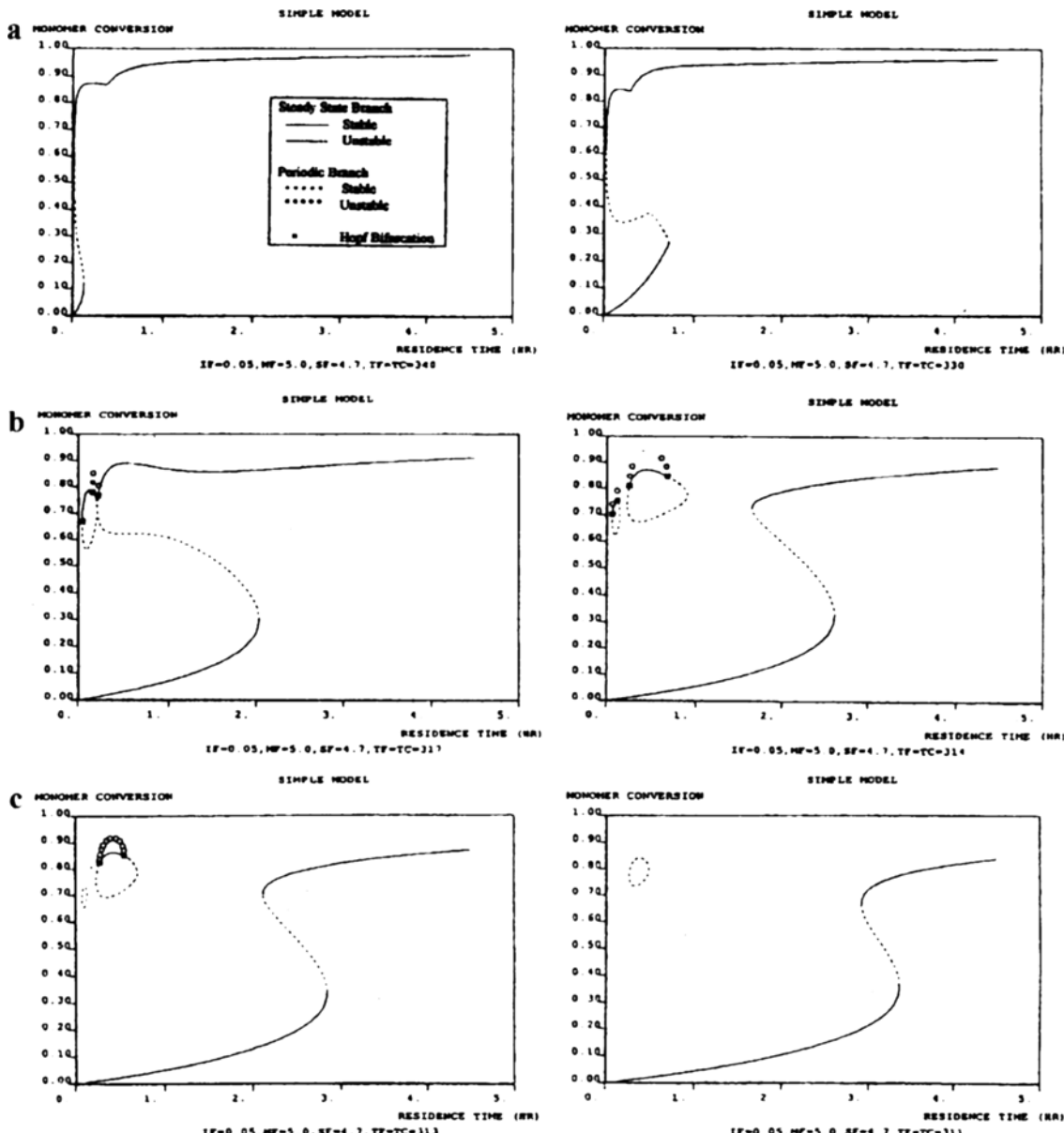


Fig. 2. Conversion steady state solution branches for selected feed temperatures for a modified simple model.

the effect of mixing on the reactor dynamics. Two isola centers shown in Table 5 were detected with varying residence time, θ , and feed temperature, T_f , as free parameters. If the feed temperature is 340 K, the conversion is high at a low residence time and three steady state solutions exist only in a narrow range at lower residence times. As the feed temperature is decreased from 340 K to 317 K, the sigmoidal curve is larger and an isola branch is cleaved from the upper solution branch of the sigmoidal curve. At a lower feed temperature, a second isola branch is pinched from the curve. The first isola branch disappears at $T_f=311$ K. These phenomena are depicted in Fig. 2. Similar behavior is observed in temperature profiles (Fig. 3). Two isola solution branches coexist and the first disappears as feed temperature decreases. Kwalik [1988] also observed two isola branches. She used the feed solvent volume fraction as the second free parameter rather than solvent concentration as used here. Consequently, the

bifurcation diagram in Fig. 3 is slightly different from that of Kwalik. Adomaitis and Cinar [1987] found multiple isola solutions in a tubular reactor, where the feedback element in a proportional control system induces the existence of multiple isola branches. Here, the nonlinearity arising from both the gel effect and the Arrhenius-type rate expressions may induce their existence.

2. Imperfect Mixing Model

2-1. Case 1 ($\kappa=0.01$, $\sigma=0.01$)

The imperfect mixing model contains two additional important parameters; the volume ratio, κ , and the exchange ratio, σ . Table 6 shows two isola centers for small values of σ and κ . The values of θ and T_f differ slightly from those of the base case, the simple model. The lower branch of steady state solutions shown in Fig. 4 is perturbed and contains a sigmoidal curve which increases as the feed temperature decreases. In contrast to the simple model, five steady states may

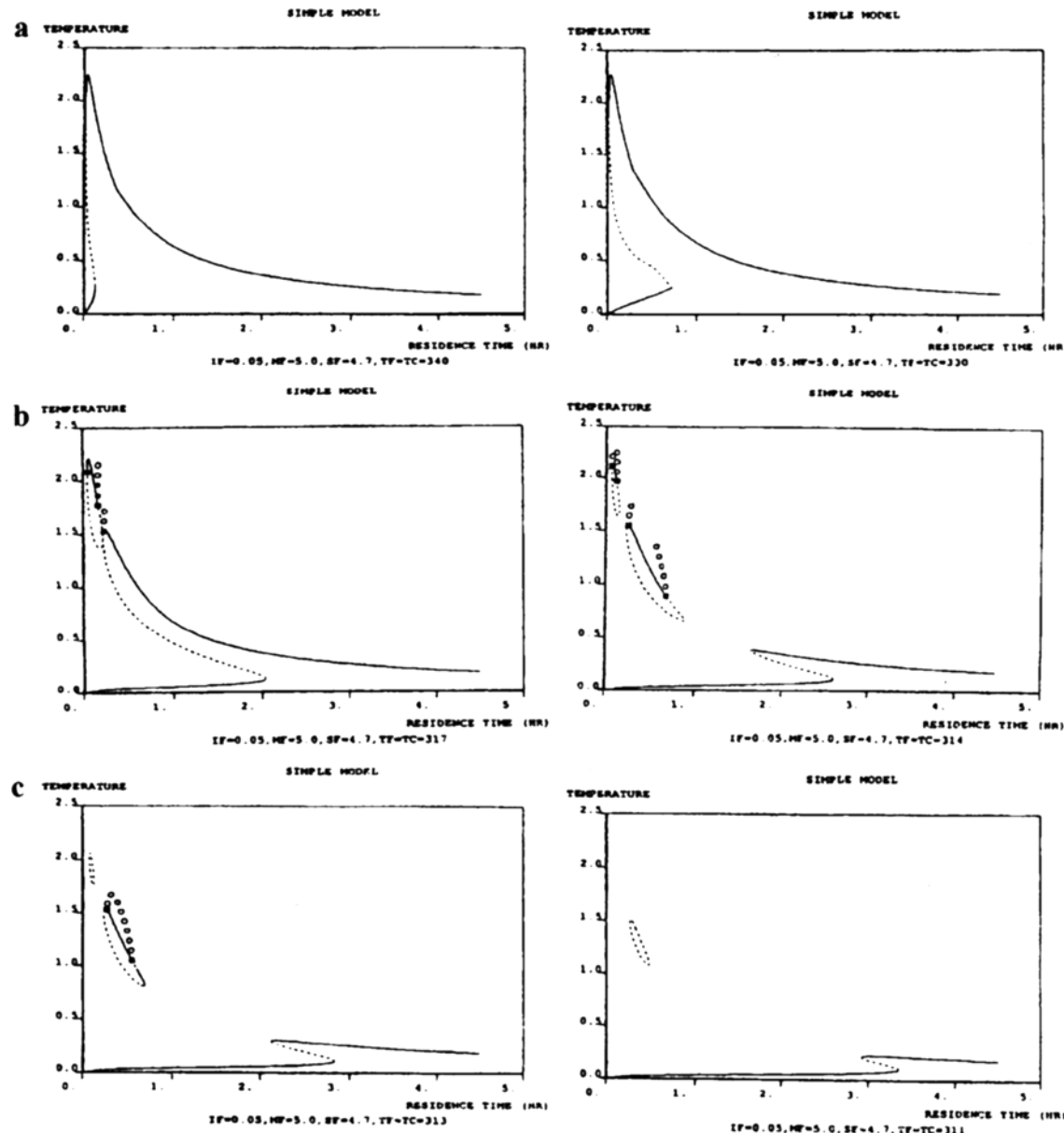


Fig. 3. Temperature solutions corresponding to the conversion branches in Fig. 2.

Table 6. Isola centers of Case 1 for an imperfect mixing model

$X_1=0.801654$	$X_2=0.2651$	$X_1=0.79253$	$X_2=0.268923$
$X_3=1.591$	$X_4=1.0$	$X_3=1.33782$	$X_4=1.0$
$X_5=1.0255 \times 10^{-6}$	$X_6=0.764498$	$X_5=4.88763 \times 10^{-6}$	$X_6=0.97831$
$X_7=0.517095$	$X_8=1.69313$	$X_7=0.920636$	$X_8=2.04005$
$X_9=1.0$	$X_{10}=5.02515 \times 10^{-7}$	$X_9=1.0$	$X_{10}=6.96577 \times 10^{-7}$
$\theta=0.0994488$	$T_F=313.267$	$\theta=0.332017$	$T_F=310.349$
Model=Imperfect		Model=Imperfect	

Fixed parameters: $I_F=0.05$, $M_F=5.0$, $S_F=4.7$, $\kappa=0.01$, $\sigma=0.01$

exist at lower residence times. The upper solution branch is not affected by the exchange between the two reactors, since the second reactor is much smaller and the limited exchange does not perturb the polymerization in the larger reactor. The temperature profiles show the same phenomena as depicted in Fig. 5.

2-2. Case 2 ($\kappa=0.01$, $\sigma=1.0$)

When the exchange ratio is increased, the positions of isola centers are almost identical to the simple model case (Table 7). The bifurcation diagrams show that the distortion of the lower branch disappears and the shape of solution branches is the same as in the simple model. The position and ampli-

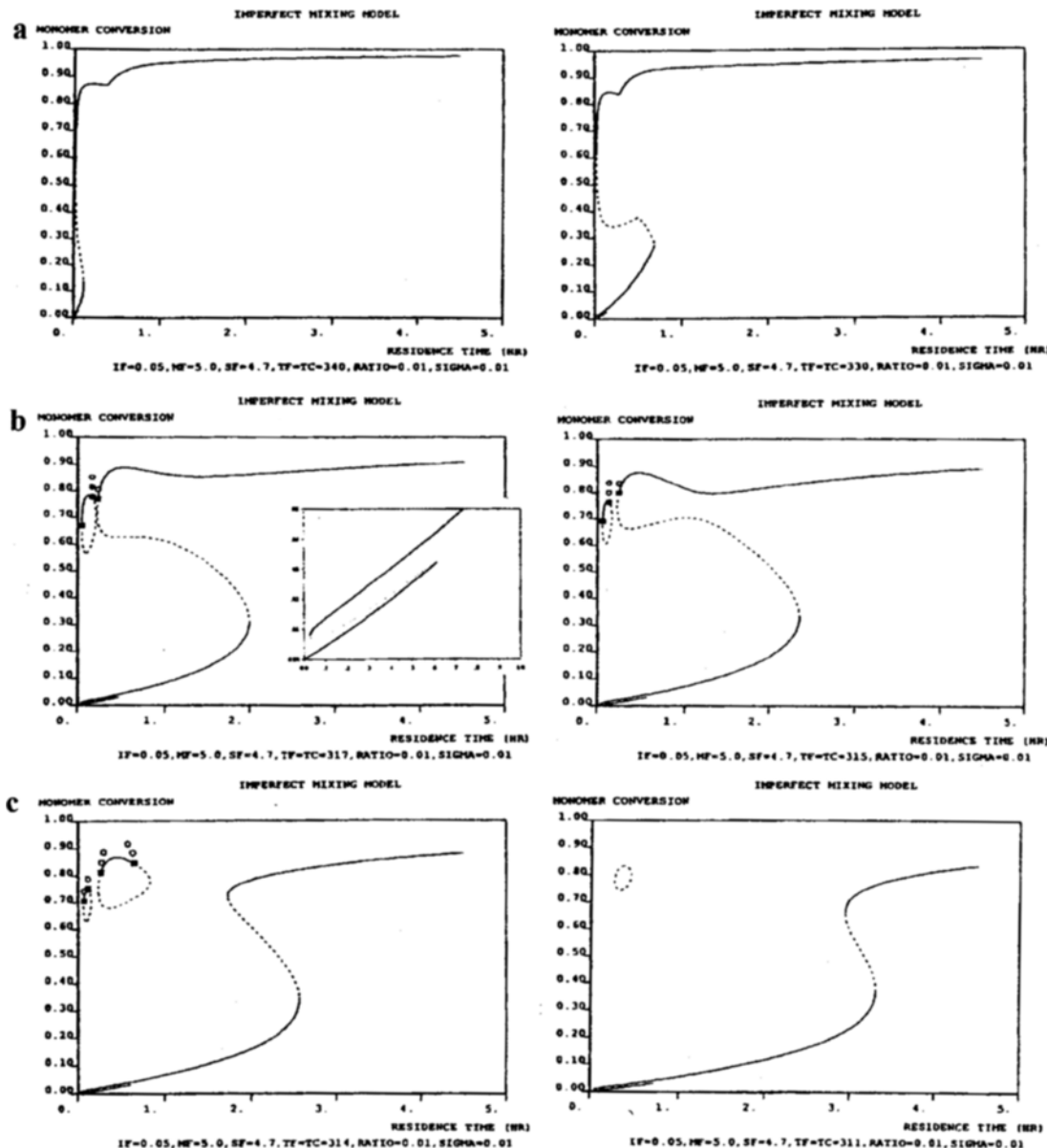


Fig. 4. Conversion steady state solution branches for selected feed temperatures in Case 1 for an imperfect mixing model.

tude of the Hopf bifurcations at the isola branches, however, are changed (Fig. 6, especially the cases of $T_f=315$ K and 314 K). We may conclude that an increase in exchange ratio does affect the dynamics of the first reactor, but as the second reactor is small, the perturbation is minor. The temperature diagrams are shown in Fig. 7 and we observe the same phenomena as in Fig. 6.

2-3. Case 3 ($\kappa=0.1$, $\sigma=0.1$)

When the volume ratio is increased ($\kappa=0.1$, $\sigma=0.1$), the positions of the isola centers differ from those in the simple model (Table 8). Only one isola branch exists at $T_f=315$ for simple model, but here two isola solutions coexist. The distortion of the lower branch of steady state solutions becomes severe with decreasing feed temperature. The region in which five steady states exist is much broader than at smaller volume ratios. These phenomena are shown in Fig. 8 and 9 for conversion and temperature, respectively. A comparison with

case (2-1) shows that increases in volume ratio and exchange ratio affect the distortion of the lower solution branch. However, since the exchange ratio is still not very large, the upper solution branch does not change.

2-4. Case 4 ($\kappa=0.1$, $\sigma=1.0$)

In this case, the positions of the isola centers (Table 9) do not change appreciably as in Case 2. At higher feed temperatures ($T_f=340$ -323 K), the bifurcation diagrams are identical to those of the simple model. At lower feed temperatures, however, the upper branch (especially the unstable steady state solution) is quite perturbed. Two Hopf bifurcation points emanate from the upper stable solution branch at $T_f=313$ K. The first appearing isola branch disappears and the distorted upper solution branch has three Hopf bifurcations for a further one degree decrease in the feed temperature. Another isola solution branch is finally cleaved from the perturbed upper branch at $T_f=311$ K. The conversion and temperature profiles

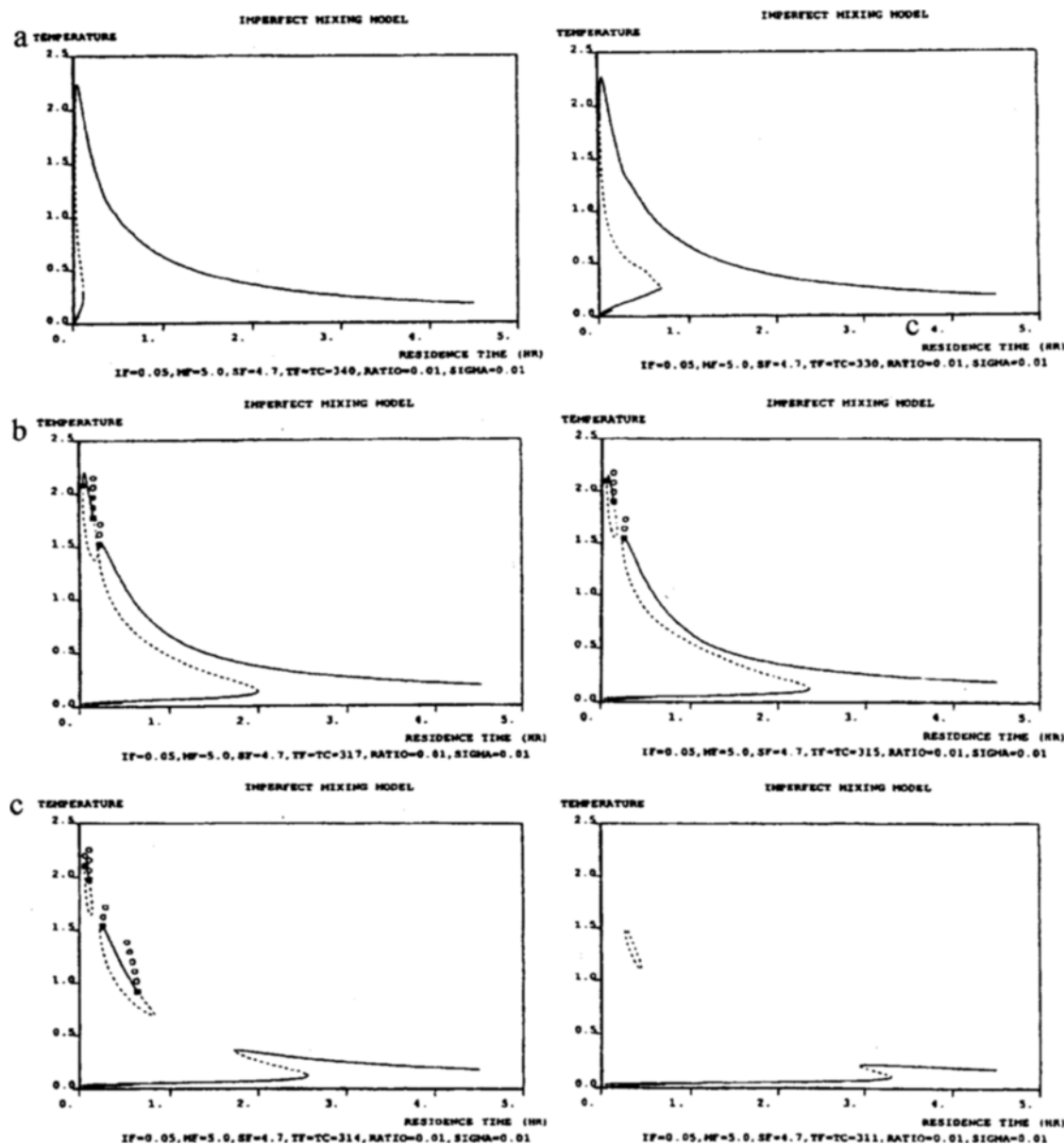


Fig. 5. Temperature solutions corresponding to the conversion branches in Fig. 4.

Table 7. Isola centers of Case 2 for an imperfect mixing model

$X_1=0.793834$	$X_2=0.259641$	$X_3=1.36142$	$X_4=1.0$
$X_5=4.94644 \times 10^{-6}$	$X_6=0.80215$	$X_7=0.262648$	$X_8=1.393$
$X_9=1.0$	$X_{10}=5.28398 \times 10^{-7}$	$T_F=309.609$	$\theta=0.328736$
Model=Imperfect			Model=Imperfect

Fixed parameters: $I_F=0.05$, $M_F=5.0$, $S_F=4.7$, $\kappa=0.01$, $\sigma=1.0$

are depicted in Fig. 10 and 11, respectively.

3. Observations

Kim [1985] studied the dynamics of coupled continuous stirred tank reactors in parallel in which an isothermal auto-catalytic reaction with a product inhibition term occurs. He examined the dynamic behavior of coupled reactors for dif-

ferent combinations such as node-focus, oscillation-focus and oscillation-oscillation. He found that for a node-focus combination, each reactor approaches a different steady state. For an oscillation-oscillation interaction, single peak oscillations, quasi-periodic oscillations and steady state operation were found at specific values of the exchange ratio. In Kim's examination

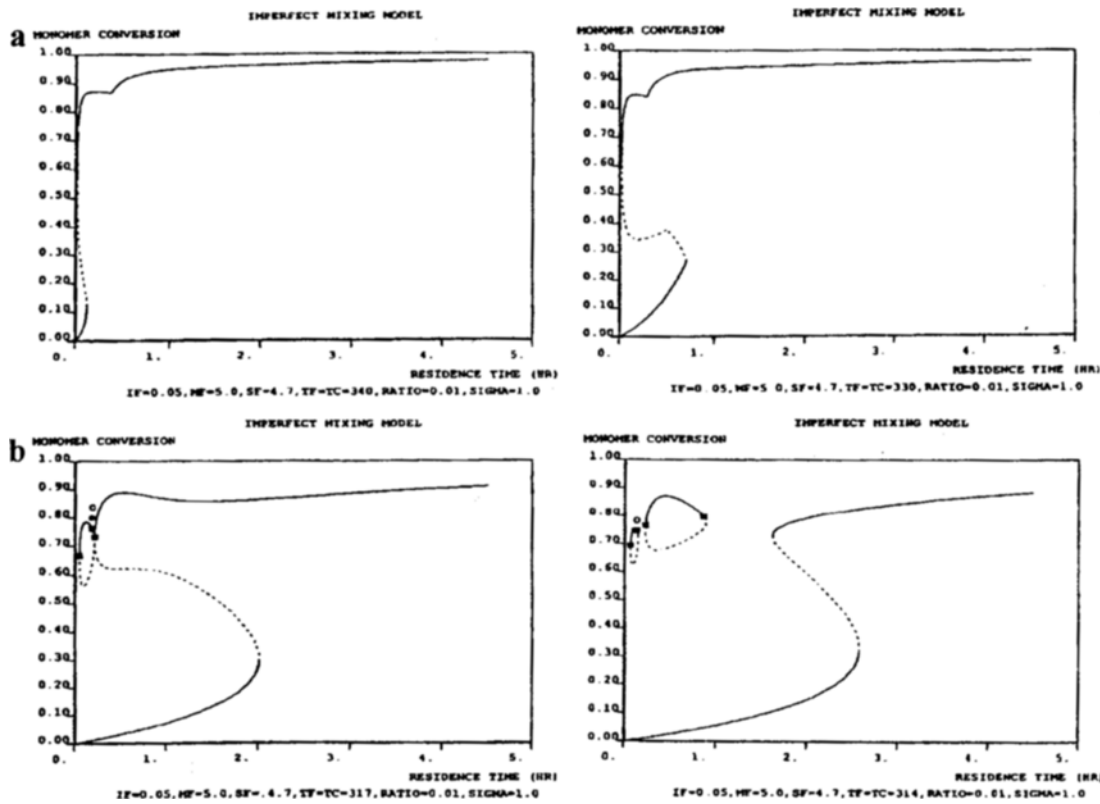


Fig. 6. Conversion steady state solution branches for selected feed temperatures in Case 2 for an imperfect mixing model.

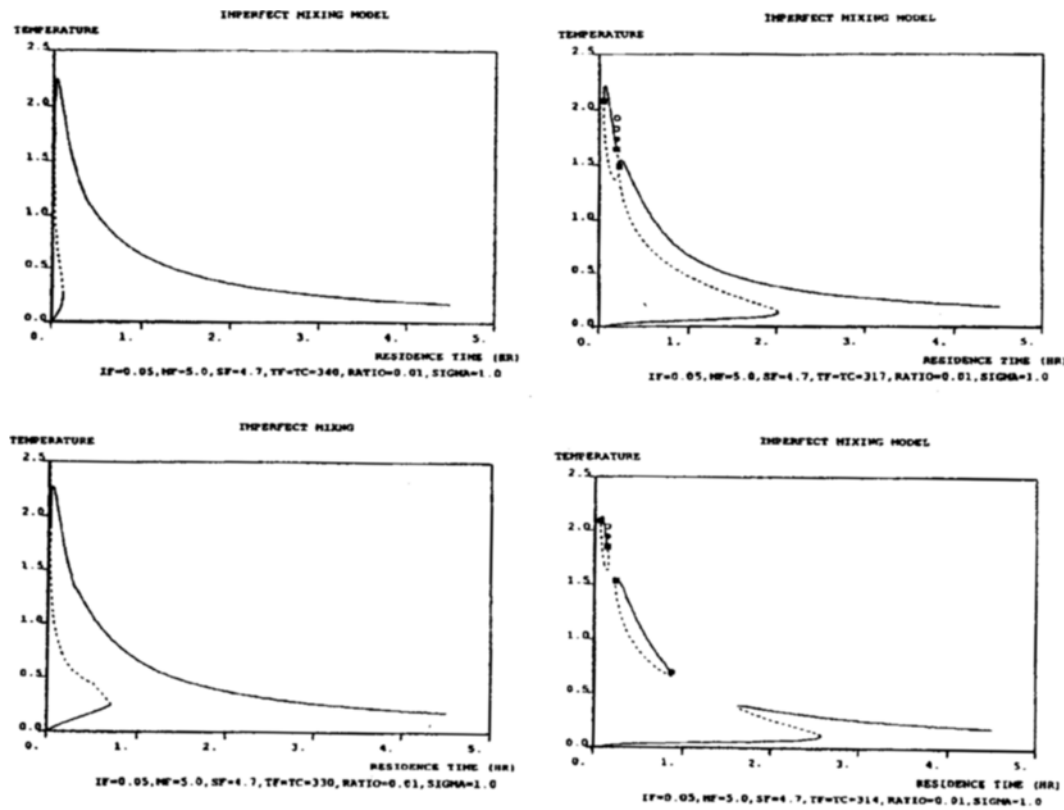


Fig. 7. Temperature solutions corresponding to the conversion branches in Fig. 6.

Table 8. Isola centers of Case 3 for an imperfect mixing model

$X_1=0.787573$	$X_2=0.281514$	$X_3=1.2883$	$X_4=1.0$	$X_5=4.74677 \times 10^{-7}$	$X_6=0.941838$	$X_7=0.409861$	$X_8=1.86188$	$X_9=1.0$	$X_{10}=2.12739 \times 10^{-7}$	$X_1=0.690134$	$X_2=0.673156$
										$X_3=1.8959$	$X_4=1.0$
										$X_5=6.89612 \times 10^{-6}$	$X_6=0.9285$
										$X_7=0.99457$	$X_8=2.77624$
										$X_9=1.0$	$X_{10}=6.54201 \times 10^{-7}$
										$\theta=0.0847368$	$T_F=313.97$
Model=Imperfect										Model=Imperfect	

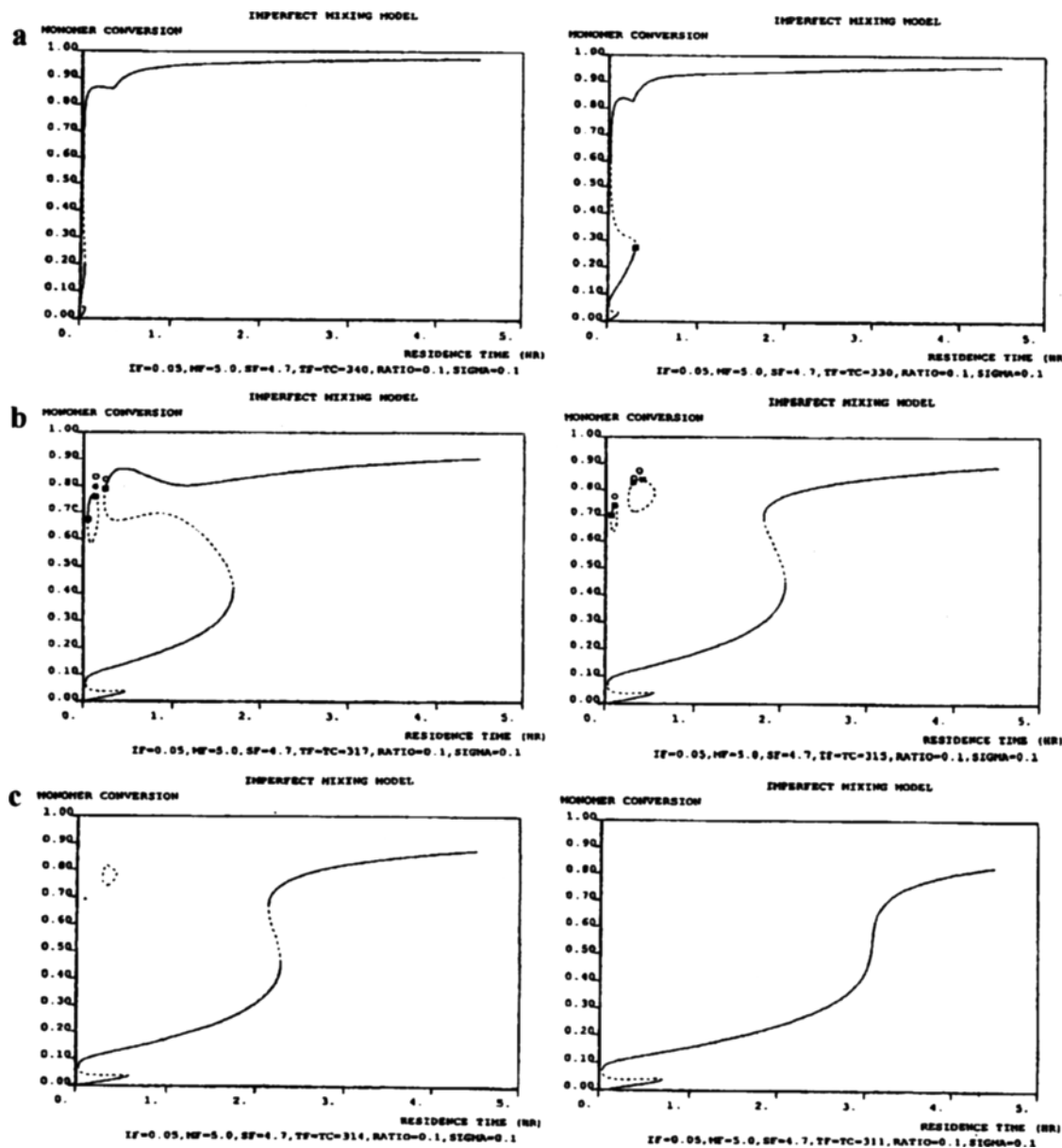
Fixed parameters: $I_F=0.05$, $M_F=5.0$, $S_F=4.7$, $\kappa=0.1$, $\sigma=0.1$ 

Fig. 8. Conversion steady state solution branches for selected feed temperatures in Case 3 for an imperfect mixing model.

of the dynamic behavior of coupled reactors in different configurations, he assumed that each reactor has the same volume and all reactors have identical feed composition. Taylor and Kevrekidis [1993] studied the dynamics of two CSTRs with individual feed, exit and coolant streams and operating in parallel. They observed that for the weakly coupled sys-

tem (exchange ratio: very small, volume ratio=1) four solutions exist (an unstable steady state, two saddle-type periodic solutions and an attracting torus).

Marini and Georgakis [1984] described that imperfect mixing has a stabilizing effect on the dynamics of a reactor for the production of low density polyethylene. Their assumptions

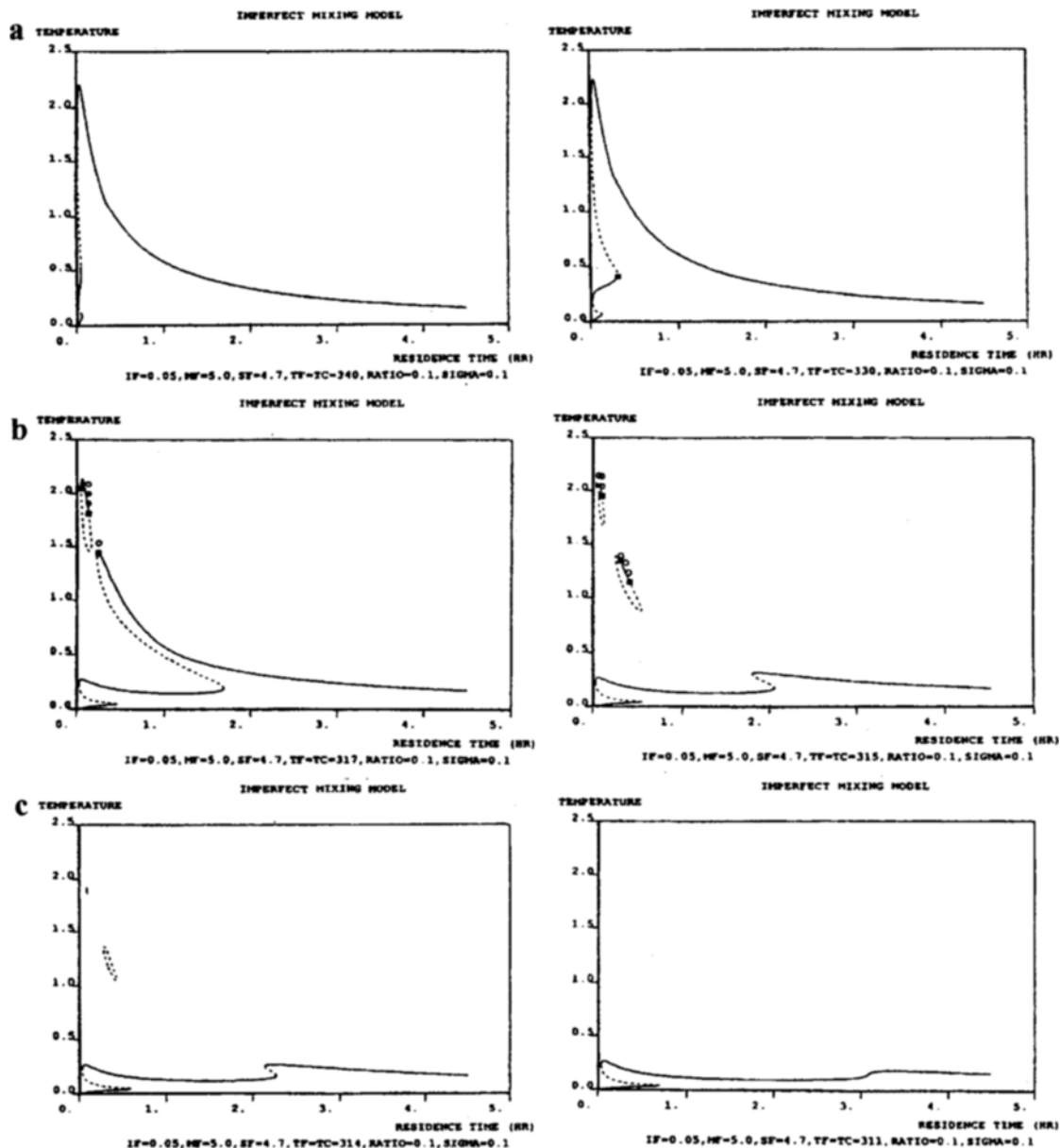


Fig. 9. Temperature solutions corresponding to the conversion branches in Fig. 8.

Table 9. Isola centers of Case 4 for an imperfect mixing model

$X_1=0.769362$	$X_2=0.26885$	$X_3=0.68399$	$X_4=0.663654$
$X_3=1.25496$	$X_4=1.0$	$X_5=1.8982$	$X_6=1.0$
$X_5=3.9855 \times 10^{-6}$	$X_6=0.884296$	$X_7=6.14661 \times 10^{-6}$	$X_8=0.783734$
$X_7=0.382728$	$X_8=1.69076$	$X_9=0.811474$	$X_{10}=2.27066$
$X_9=1.0$	$X_{10}=9.31511 \times 10^{-7}$	$X_{10}=1.0$	$X_{10}=1.10585 \times 10^{-6}$
$\theta=0.325907$	$T_F=309.865$	$\theta=0.0850214$	$T_F=312.245$
Model=Imperfect		Model=Imperfect	

Fixed parameters: $I_F=0.05$, $M_F=5.0$, $S_F=4.7$, $\kappa=0.1$, $\sigma=1.0$

were (i) that the vessel is divided into two small CSTRs in series (3-5 % of total volume) and one CSTR accounting for the remaining volume where most of the reaction occurs, and (ii) that the exchange ratio is large (greater than one). However, they did not study the dynamics of an imperfect

mixing model. Kim et al. [1991] studied the dynamics of a cascade of two continuous stirred tank polymerization reactors with a binary initiator mixture. They found, using the reactor residence time as a bifurcation parameter, that the second reactor has five steady states.

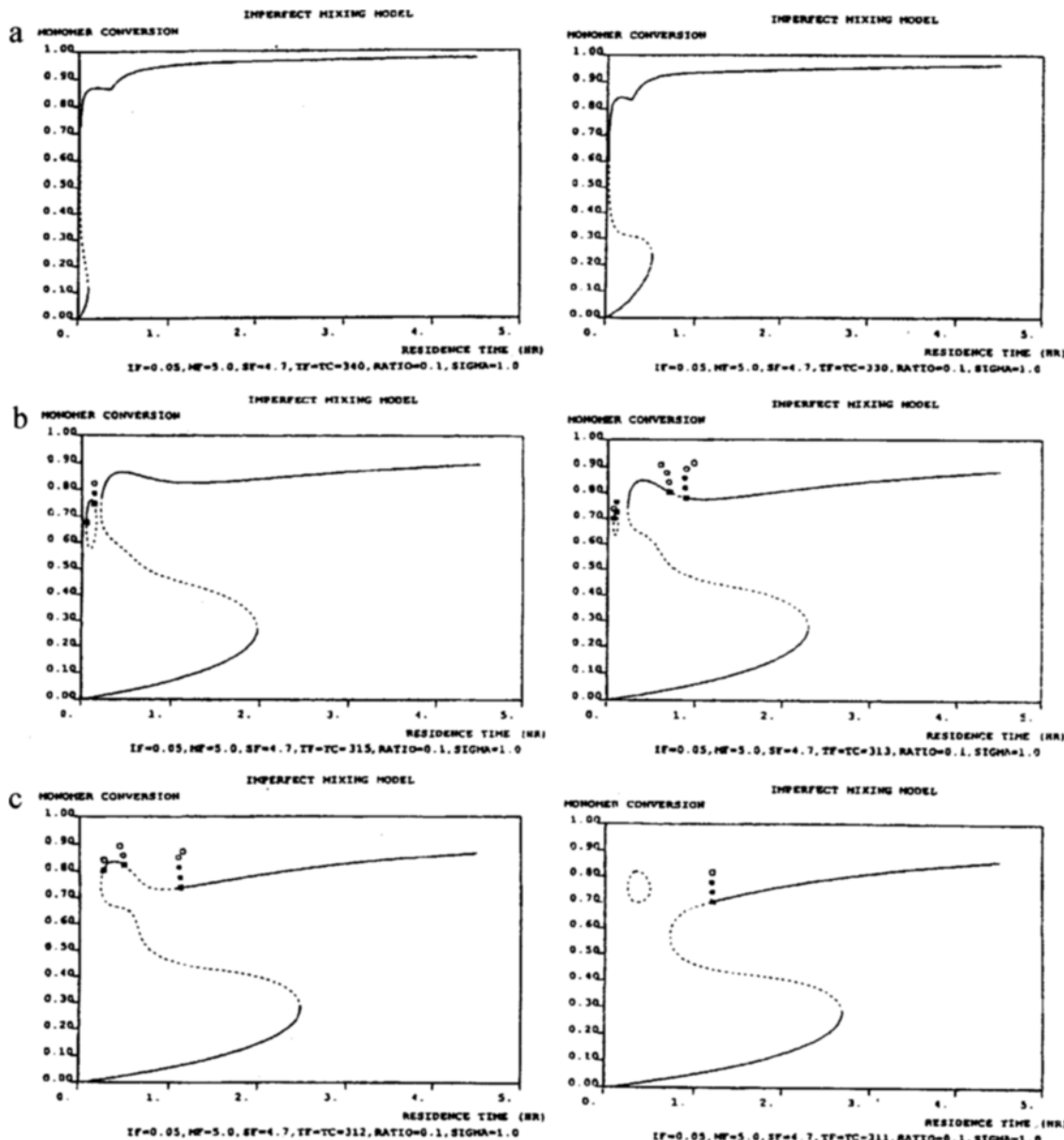


Fig. 10. Conversion steady state solution branches for selected feed temperatures in Case 4 for an imperfect mixing model.

In this work, the volume of the second reactor is small (1-10 % of total reactor volume) and the reactor does not have feed inflow and product discharge. In case 2, we observed that the dynamics of the first reactor is slightly destabilized by the second. The stable steady state region on the isola branch is reduced in comparison to the case of perfect mixing. In case 4, we found that the upper solution branch is distorted and three Hopf bifurcations occur. Phenomena such as period-doubling and torus formation are not observed. For the weakly coupled cases (case 1, 3), five steady states were found at lower residence times. In summary, for small volume ratios and exchange ratios, the lower solution branch is distorted and five steady states exist in a specific region. On the other hand, for small volume ratios and medium exchange ratios, the upper branch of steady state solutions differs from

those for the case of the simple model.

Steady state solutions differ from those in the simple model because conversion and reaction temperature in the second reactor (small size) are greater than those in the main tank (As an example, case 3 is depicted in Fig. 12). Due to the exchange of mass and energy between both reactors, more heat may be transferred to the first tank. The unreacted monomer may not travel to the first reactor, since the monomer is almost completely consumed at very small residence time. The energy transfer does perturb the dynamics of the first tank. Such a phenomenon was similarly observed by Mankin and Hudson [1986], studying two continuous stirred tank reactors, each with exothermic chemical reaction, coupled by heat and mass transfer. Note that the second reactor does not efficiently transfer heat of reaction to the wall. Since we con-

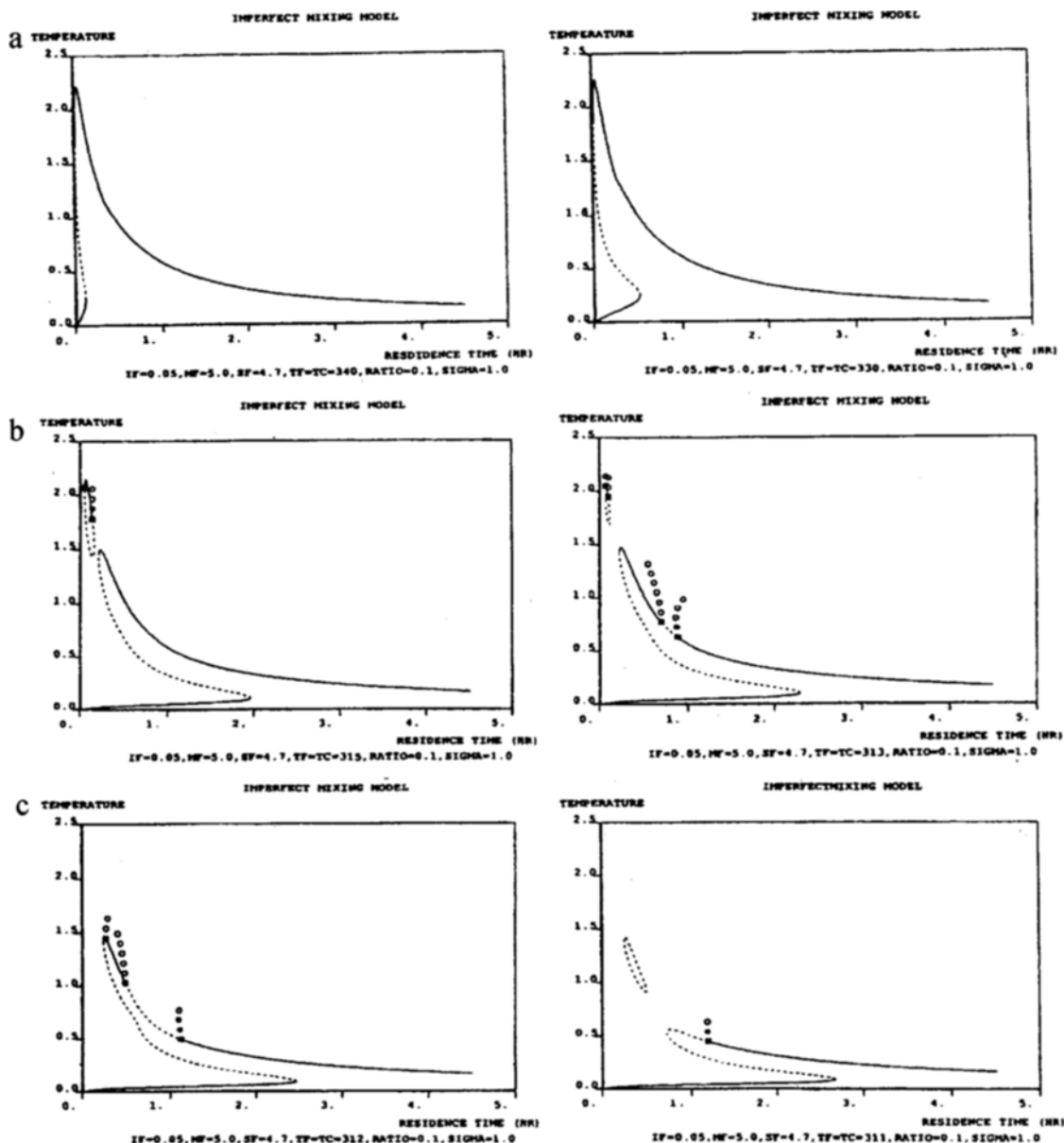


Fig. 11. Temperature solutions corresponding to the conversion branches in Fig. 10.

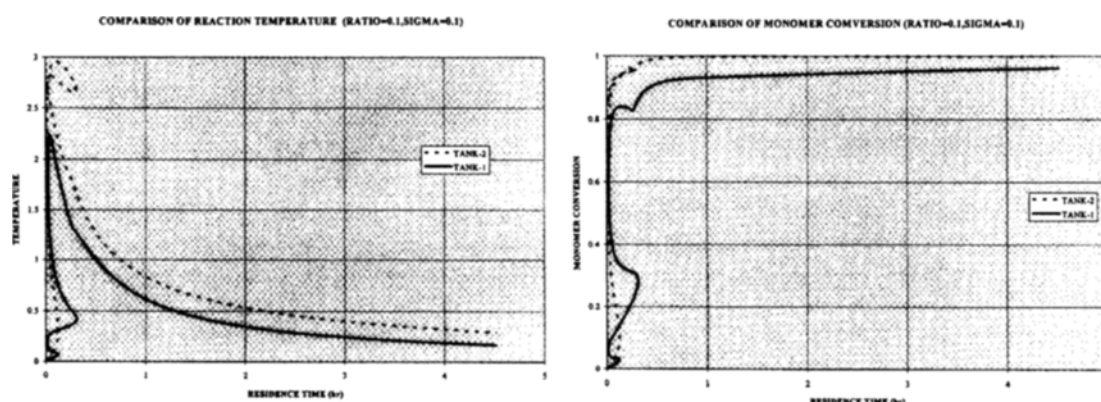


Fig. 12. A comparison of conversion and temperature in two tanks.

sider an imperfect mixing model in which mixing near the agitator differs from the rest of the reactor, mass and energy

in the second tank (the region near the agitation) are exchanged only with the first tank.

CONCLUSION

In order to develop a better general understanding of dynamics of MMA polymerization reactors, to better control polymer properties, and to improve productivity, two models have been developed, one accounting for imperfect mixing and the second, detailed model involving fewer assumptions. A configuration of two-tanks-in-parallel was used to study the effect of mixing on the reactor dynamics. The model includes two parameters, i.e., the exchange ratio, σ , and the volume ratio, κ .

1. If two ratios are small ($\kappa=0.01$, $\sigma=0.01$), the lower branch of steady state solutions is perturbed when compared to a simple model which assumes perfect mixing. Two sigmoidal curves of solutions are observed.

2. As σ increases further ($\kappa=0.01$, $\sigma=1.0$), the shape of the solution branches is the same in a simple model, but the position and amplitude of the Hopf bifurcations at the isola solution branch were changed.

3. When volume ratio is large ($\kappa=0.1$, $\sigma=0.1$), the distortion of the lower branch of the steady state solutions becomes more severe with decreasing feed temperature.

4. If σ is also large ($\kappa=0.1$, $\sigma=1.0$), the shape of steady state solutions is very different from that of a simple model. The upper solution branches are more perturbed as feed temperature decreases.

NOMENCLATURE

A_r	: total heat transfer area
C_p	: heat capacity
D_{ai}	: Damköhler number, $i=I, P, T$
E_i	: activation energy of species i
f	: initiator efficiency factor
$(-\Delta H_p)$: heat of reaction
I	: initiation concentration
k_d	: rate constant for initiation
k_f	: rate constant for chain transfer, $i=M, S$
k_p	: rate constant for propagation
k_t	: rate constant for termination
M	: monomer concentration
q_r	: exchange flow rate
RATIO	: volume ratio (κ in Table 2)
S	: solvent concentration
SIGMA	: flow exchange ratio (σ in Table 2)
T	: reaction temperature
T_c	: coolant temperature
t	: time
U	: overall heat transfer coefficient
V	: reactor volume
X_i	: dimensionless variables defined in Table 2

Greek Letters

β	: dimensionless variable defined in Table 2
γ	: dimensionless variable defined in Table 2
σ	: flow exchange ratio
κ	: volume ratio defined in Table 2

ϕ_i : volume fraction of species i

θ : residence time

τ : dimensionless time

Subscripts

c	: coolant
d	: initiator
f	: feed
p	: polymer
r	: recycle
s	: solvent

REFERENCES

Adebekun, A. K., Kwalik, K. M. and Schork, F. J., "Steady-State Multiplicity During Solution Polymerization of Methyl Methacrylate in a CSTR", *Chem. Eng. Sci.*, **44**(10), 2269 (1989).

Adomaitis, R. A. and Cinar, A., "The Bifurcation Behavior of an Autothermal Packed Bed Tubular Reactor", American Control Conference, Minneapolis, MN, p.1419 (1987).

Baillagou, P. E. and Soong, D. S., "Major Factors Contributing to the Nonlinear Kinetics of Free-Radical Polymerization", *Chem. Eng. Sci.*, **40**(1), 75 (1985).

Balakotaiah, V. and Luss, D., "Structure of Steady-State Solutions of Lumped Parameter Chemically Reacting Systems", *Chem. Eng. Sci.*, **37**, 11 (1982).

Chen, M. S. K. and Fan, L. T., "A Reversed Two-Environment Model for Micromixing in a Continuous Flow Reactor", *Can. J. Chem. Eng.*, **49**, 704 (1971).

Choi, K. Y., "Analysis of Steady State of Free Radical Solution Polymerization in a Continuous Stirred Tank Reactor", *Polym. Eng. Sci.*, **26**(14), 975 (1986).

Doedel, E., "AUTO: Software for Continuation and Bifurcation Problems in Ordinary Differential Equations", Cal-Tech., Pasadena (1986).

Hamer, J. W., Akramov, T. A. and Ray, W. H., "The Dynamic Behavior of Continuous Polymerization Reactors-II: Nonisothermal Solution Homopolymerization and Copolymerization in a CSTR", *Chem. Eng. Sci.*, **36**(12), 1897 (1981).

Kafkas, G. A., "Experimental Studies and Mathematical Modeling of Aqueous Suspension Polymerization Reactors", Ph. D. Thesis, Univ. of Wisconsin, Madison (1992).

Kim, K. J., Choi, K. Y. and Alexander, J. C., "Dynamics of a Cascade of Two Continuous Stirred Tank Polymerization Reactors with a Binary Initiator Mixture", *Poly. Eng. Sci.*, **31**(5), 333 (1991).

Kim, S., "Application of Nonlinear Dynamic Analysis to Chemically Reacting Systems", Ph. D. Thesis, State Univ. of New York, Buffalo (1985).

Kiparissides, C., Sidiropoulou, E., Voutetakis, S. and Froussakis, C., "Control of Molecular Weight in a Batch Polymerization Reactor Using Long-Range Predictive Control Methods", *Chem. Eng. Comm.*, **92**, 1 (1990).

Kubicek, M. and Marek, M., "Computational Methods in Bifurcation Theory and Dissipative Structures", Springer-Verlag, NY (1983).

Kwalik, K. M., Adebekun, A. K. and Schork, F. J., "Closed-

Loop Bifurcation, Estimation and Control of a Continuous Solution Polymerization Reactor", in K. H. Reichert and H. Geissler ed., *Polymer Reaction Engineering*, VCH, p. 123 (1989).

Kwalik, K. M., "Bifurcation Characteristics in Closed-Loop Polymerization Reactors", Ph. D. Thesis, Georgia Institute of Technology, GA (1988).

Louie, B. M. and Soong, D. S., "Optimization of Batch Polymerization Processes-Narrowing the MWD. 1. Model Simulation", *J. Appl. Polym. Sci.*, **30**, 3707 (1985).

Mankin, J. C. and Hudson, J. L., "The Dynamics of Coupled Nonisothermal Continuous Stirred Tank Reactors", *Chem. Eng. Sci.*, **41**(10), 2651 (1986).

Marini, L. and Georgakis, C., "Low-Density Polyethylene Vessel Reactors: Part I. Steady State and Dynamic Modelling", *AIChE J.*, **30**(3), 401 (1984).

Moritz, H. U., "Increase in Viscosity and Its Influence on Polymerization Processes", *Chem. Eng. Technol.*, **12**, 71 (1989).

Ross Jr., R. T. and Laurence, R. L., "Gel Effect and Free Volume in the Bulk Polymerization of Methyl Methacrylate", *AIChE Symp. Ser.*, **160**(72), 74 (1976).

Taylor, M. A. and Kevrekidis, I. G., "Couple, Double, Toil and Trouble: A Computer Assisted Study of Two Coupled CSTRs", *Chem. Eng. Sci.*, **48**(11), 2129 (1993).

Teymour, F. A. R. and Ray, W. H., "The Dynamic Behavior of Continuous Stirred Tank Reactor. IV. Dynamic Stability and Bifurcation Analysis of an Experimental Reactor", *Chem. Eng. Sci.*, **44**(9), 1967 (1989).

Thiele, R. and Breme, J., "Micro- and Macromixing in Polymerization Reactors", *Intern. Polymer Processing III*, **1**, 48 (1988).

Thiele, R., "The Interaction Between Process Design and Mechanical Design in Development of Mass Polymerization Reactors", in K. H. Reichert and H. Geissler ed., *Polymer Reaction Engineering*, VCH, p.399 (1989).

Tosun, G., "A Mathematical Model of Mixing and Polymerization in a Semibatch Stirred-Tank Reactor", *AIChE J.*, **38**(3), 425 (1992).

Uppal, A., Ray, W. H. and Poore, A. B., "On the Dynamics Behavior of Continuous Stirred Tank Reactors", *Chem. Eng. Sci.*, **29**, 967 (1974).

Uppal, A., Ray, W. H. and Poore, A. B., "The Classification of the Dynamic Behavior of Continuous Stirred Tank Reactors-Influence of Reactor Residence Time", *Chem. Eng. Sci.*, **31**, 205 (1976).

Villemaux, J., "A Simple Model for Partial Segregation in a Semibatch Reactor", Paper 114a, AIChE Meeting, San Francisco (1989).

Villemaux, J., "Micromixing Phenomena in Stirred Reactors", in *Encyclopedia of Fluid Mechanics*, Gulf Pub., Houston, p.707 (1986).